

Iris Verification System Based on Curvelet Transform

Hanene Guesmi^{*(1,2)}, Hanene Trichili^(1,2), Adel M. Alimi⁽¹⁾, Basel Solaiman⁽²⁾

⁽¹⁾ REGIM: REsearch Group on Intelligent Machines

National engineering School of Sfax (Tunisia)

⁽²⁾ Department of Image and Information Processing (ITI)

Telecom-Bretagne, Brest – France

guesmi.hanen@ieee.org, hanene.trichili@telecom-bretagne.eu, adel.alimi@ieee.org, basel.solaiman@telecom-bretagne.eu

Abstract-- The performance of the iris verification process highly depends on its extractor of iris features. So, to reduce the dimensionality of the iris image and improve the recognition rate, an iris features extraction method based on curvelet transform is proposed and presented in this paper. Thus, our paper focuses on presenting of our curvelet-based iris features extraction method. This method consists of two steps: decompose images into set of sub-bands by the curvelet transform and automatic extraction of the most discriminative features of these sub-bands. An extensive experimental results show that the proposed method is effective and encouraging.

Key words component-- Features extractions, Iris verification, Curvelet transform

I. INTRODUCTION

The iris recognition has been the subject of intensive research for almost two decades. A large number of research papers and reports have already been published on iris recognition. In 1994, Daugman patented its first algorithm of iris recognition. In this algorithm, the features iris extraction phase was the key to the success of this algorithm. Thus, to successfully recognize an iris, it must be well represented by a set of relevant features. So, this representation is based on discriminative descriptors which can extract from the iris image. In the literature, many approach of encoding iris was proposed. In the first iris recognition system, Daugman [7] used the Gabor filter to encode the normalized iris. Gabor filter was used, also, by many others research works like C.Sanchez-Avila et al. [1]. In the second iris recognition system invented and patented by Wildes et al. [18], the decomposition of Laplacian pyramid was integrated in his features iris extraction method.

W. W. Boles et al. [3] proposed an extractor of iris features based on Zero-crossing representation of the 1D signal of the normalized iris. This representation is obtained while being based on the Wavelets transform. Also, iris decomposition into Wavelets packages was proposed by Rossant et al. [19] to encode iris.

The Hidden Markov Model was used in the encoding iris by Wang Tong et al. [17]. The authors estimate a probability

score in the modeling HMM phase by the comparison of the HMM normalized iris and the HMMs of the training irises.

Another research choose to encode iris on base of statistical features like Nabti et al. [14] who calculated the 7 invariant moments to generate an iris features vector. Also, in [9], the authors proposed to extract the some statistical features of the iris circles in order to encode an iris. Amir Azizi et al. [2] used Haralicks coefficients [8] which are extracted from co'occurrences matrixes of the set of directional sub-bands decomposed by the contourlet.

In this framework, we propose a novel iris features extraction method based on curvelet transform. Curvelet transform has shown good results in content based image retrieval [16], character recognition [11], and face recognition [12] etc. For this fact, we have chosen to integrate a curvelet transform in our iris features extraction method. Some curvelet Statistical descriptors were derived from the sub-bands generated by the curvelet decomposition of the normalized iris. So, the remainder of our paper is organized as follows: Section 2 describe the curvelet transform approach. In Section 3, we present our iris verification process which is based on the curvelet transform which is used in our novel features iris extraction method. Then we present the experiment results of the evaluation of our method in section 4. Finally, concluding remarks are given in Section 5.

II. CURVELET TRANSFORM

Curvelet transform is a geometric transform developed by Emmanuel Candes et al. [5] to overcome the inherent limitations of wavelet like transforms. Curvelet transform is a multi-scale and multi-directional transform with needle shaped basis functions. Basis functions of wavelet transform are isotropic and thus it requires large number of coefficients to represent the curve singularities. Curvelet transform basis functions are needle shaped and have high directional sensitivity and anisotropy. Curvelet obey parabolic scaling. Because of these properties, curvelet transform allows almost optimal sparse representation of curve singularities [5]. The curvelet transform at different scales and directions span the entire frequency space. So, curvelet transform was designed to represent edges and other singularities along curves much more efficiently than traditional transforms, i.e., using fewer coefficients for a given accuracy of reconstruction.

Curvelet transform is a ridge transform added with binary square window [8], which means subdividing a curve into approximate straight enough to carry out ridge transform. However, there exists big data redundancy in the transform. Therefore, improving the first generation curvelet transform can obtain the 2nd generation, and the second takes on features of faster computation and less redundancy. First, define x as space position parameter, w as frequency domain parameter and (r, θ) as polar frequency domain in the 2-dimensional space R^2 . $W(r)$ and $V(r)$ are smooth non-negative “radius window” and “corner window” respectively, and they must satisfy:

$$\sum_{j=-\infty}^{\infty} W^2(2^j r) = 1, r \in \left(\frac{3}{4}, \frac{3}{2}\right) \quad (1)$$

$$\sum_{j=-\infty}^{\infty} V^2(2^j r) = 1, r \in \left(-\frac{1}{2}, \frac{1}{2}\right) \quad (2)$$

For all scales $j \geq j_0$, define its Fourier frequency domain window:

$$U_j(r, \theta) = 2^{-\frac{3j}{4}} W(2^{-j} r) V\left(\frac{2^{j/2} \theta}{2\pi}\right) \quad (3)$$

Frequency domain curvelet transform is defined as product of $\varphi_{j,l,k}$ and $f \in L^2(R^2)$.

$$c(j, l, k) = \langle f, \varphi_{j,l,k}(x) \rangle = \int_{R^2} f(x) \overline{\varphi_{j,l,k}(x)} dx \quad (4)$$

$$\begin{aligned} c(j, l, k) &:= \frac{1}{(2\pi)^2} \int \hat{f}(w) \overline{\varphi_{j,l,k}(w)} dw \\ &= \frac{1}{(2\pi)^2} \int \hat{f}(w) U_j(R_{\theta_L} w) \exp[i\langle x_k^{(j,l)}, w \rangle] dw \end{aligned}$$

Curvelet also include components on rough and fine scale, the same as wavelet theory. Introduce a low-pass window W_0 , which satisfies:

$$|W_0(r)|^1 + \sum_{j \geq 0} |W_0(r)|^2 = 1, (k_1, k_2) \in Z \quad (5)$$

Define curvelet on rough scale:

$$\varphi_{j_0,k}(x) = \varphi_{j_0}(x - 2^{-j_0} k) \quad (6)$$

$$\hat{\varphi}_{j_0,k}(x) = 2^{-j_0} W_0(2^{-j_0} |w|) \quad (7)$$

So, curvelet on rough scale is non-directional. The whole of curvelet transform is composed of directional components on fine scale and isotropic wavelet on rough scale. The implementation of curvelet transform can be summarized by the following steps:

i. Sub-band Decomposition: The image is decomposed into $\log_2 M$ (M is the size of the image) wavelet sub-bands. Then, the curvelet Sub-bands are formed by performing partial reconstruction from these wavelet sub-bands at levels $j \in \{2s, 2s+1\}$. Thus the curvelet Sub-band, $s = 1$ corresponds to wavelet sub-bands $j = 0, 1, 2, 3$, curvelet Sub-band, $s = 2$ corresponds to wavelet sub-bands $j = 4, 5$ and so on.

ii. Smooth Partitioning: Each sub-band is subdivided into an array of overlapping blocks.

iii. Renormalization: Each square resulting in the previous stage is renormalized to unit scale.

iv. Ridgelet Analysis: Ridgelet transform [4] is performed on each square resulting from the previous while being follow these steps:

- ✓ Compute the 2-D Fast Fourier Transform (FFT) of the image.

- ✓ Perform cartesian to polar conversion. This is achieved by substituting the sampled values of the Fourier transform obtained on the square lattice with the sampled values on a polar lattice.
- ✓ Compute the 1-D inverse FFT on each angular line.
- ✓ Apply wavelet transform on the resulting angular lines in order to obtain the ridgelet coefficients.

The construction of curvelet basis obeys the anisotropic (parabolic) scaling relation between its length and width (length $\approx 2^{-j/2}$, width $\approx 2^{-j}$) [6]. In addition, the curvelet basis is oscillatory in one direction (x_1) and as low-pass filter in other direction (x_2). At fine scale 2^{-j} , a curvelet is a little needle shaped basis whose envelope is a specified ridge of effective length $2^{-j/2}$ and width 2^{-j} which display oscillatory behavior across the irregular main ridge [6]. On the other hand, Iris image contains intrinsic geometrical structures i.e. rings, concentric furrows, radial furrows, freckles etc. Also, Iris pattern exhibits irregular blocks (pigment spots), raised linear ridges, and tiny crypts which are slightly darker than their surrounding areas (leads to oscillatory pattern). In effect, these iris features will be represented effectively by the use of curvelet transform and due to parabolic scaling, curvelet transform extracts the aforementioned geometrical iris structures and provide optimal sparse representation with very high directional sensitivity and anisotropy for iris features.

III. OUR IRIS VERIFICATION PROCESS

In the figure Fig.1 we present the chart flow of the test phase of our iris verification process. In this process, firstly, we proceed to localize an iris in the eye image. For this fact, we have used the Masek's [13] method based on the methodology suggested on [18]. In this method, a binary edge image map will be constructed by using the Kovess [10] edge detector which analyzed a variation of the well known Canny edge detector. Then, the circular Hough transform was applied on the binary edge image map in order to determine the iris/sclera border and the pupil border. This methodology was included on several iris segmentation approaches proposed in the literature. Secondly, in iris normalization step, the process involves unwrapping the iris image and converting it into its polar equivalent. It is carried out by using Daugman's Rubber sheet model [7]. Then we encode the normalized iris on base of curvelet transform. Finally we generate the decision of our iris verification system in matching and decision step.

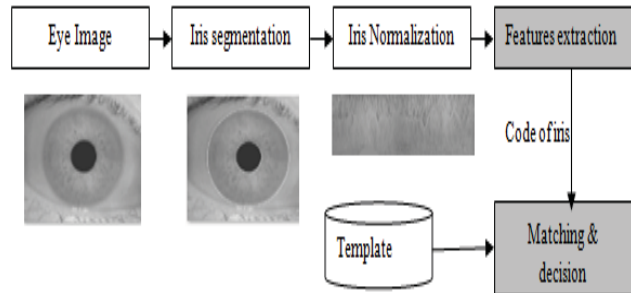


Fig. 1: Chart Flow of our iris verification process (Test phase)

A. Our Iris features extraction method based on Curvelet transform

Previous research in multi-resolution texture analysis [15] suggests some statistical descriptors: energy, entropy, mean, and standard deviation to be applied on the curvelet sub-bands in order to represent an image. Encouraging results were presented in these research works which have extracted these descriptors from texture which was decomposed by curvelet transform. These results encouraged us to integrate this approach in our features iris extractor.

So, the structural activity extracted from the curvelet transform of the image can be analyzed statistically to generate iris features vector. Thus, we have applied the curvelet transform on the normalized and enhanced iris. The curvelet decomposition generate several sub-bands images. Then, we calculate the statistical features from all these sub-bands to generate the iris features vector. In the following figure (Fig.2) we present our iris encoding method.

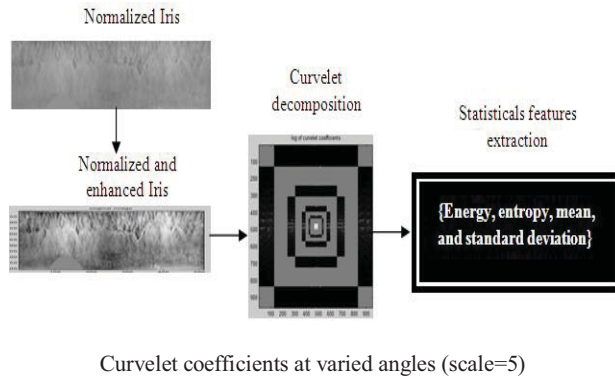


Fig. 2 Schematic diagram of a proposed iris features extraction method.

If a given iris image of size 512×512 is decomposed into 5 scales, thus the number of the directional sub-bands images varies from scale to scale. So, we will have 32 sub-bands images at second scale and at scales 3 and 4 we will have 64 sub-bands images. So, extracting features from these sub-bands images and representing in a compact form is a major problem. To overcome this problem, we encode each sub-band image by 4 statistical features (Energy, entropy, standard deviation, and mean). Thus, in the totality, we have in the first scale one sub-band which is coded by four features values, in the second scale we have thirty two sub-bands which are coded by 32×4 features values. In the third scale, we get 64 sub-bands which are coded by 64×4 features values. Also, the follow scale, we get 64×4 features values. Finally, in the fifth scale, we get one sub-band which is coded by 1×4 features values. A result, we obtain 164×4 features values to encode the normalized iris. Thus, our features vector contains 4 rows. Each row contains 164 values of a feature (energy, entropy, mean or standard deviation) extracted from 164 sub-bands.

It is desirable to obtain an iris representation invariant to translation, scale, and rotation. The scale and translation effects are removed in normalization and segmentation, respectively. The rotation invariance is achieved by converting the iris ring into rectangular fixed block of size 64×512 with seven initial angles $-9^\circ; -6^\circ; -3^\circ; 0^\circ; 3^\circ; 6^\circ; 9^\circ$. We thus define seven templates which, respectively, denote the seven rotation angles for each iris class in the database.

When matching the input feature vector with the templates of a class, the minimum of the seven scores is taken as the final matching score.

B. Matching and decision step

In the matching and decision step, we calculate the Euclidian distances between the rows of features vectors of the tow irises. We achieve four Euclidian distances. Then, we calculate the norm of these distances. We take this norm as a dissimilarity score. Thus, this score would be compared with a given threshold. If this score is lower than the threshold, we accept this iris and we considerate that is a genuine individual.

IV. EXPERIMENTS RESULTS

In this section, we present the results of the evaluation of our iris verification system based on curvelet transform. The performance of our method is validated using the iris CASIA databases (version 1.0 and version 2.0 (device 1))[20]. The CASIA Version 1.0 database contains 756 eye images of 108 individuals: 4×108 irises are used for training and 3×108 irises are used for test. The images of CASIA Database Version 2.0 have been captured with different instruments under varying conditions and different ethnicity. CASIA Database Version 2.0 includes two subsets captured with two different devices: Each subset includes 1200 images from 60 classes. We have divided the device1 sub-set into two other sub-sets: the training data set containing 60×12 images, and the test data set containing 60×8 images.

The implemented algorithm for the comparison is the Daugman's algorithm [7]. This algorithm is the most efficient in the literature and the first patented algorithm. The Gabor filter was used to encode the normalized iris. Thus, the normalized iris is used to obtain 2,048-bits IrisCode. The dissimilarity score between two IrisCodes is estimated using Hamming distance.

To evaluate our iris method verification, we have measure the computational time and the error rates. So, the average computational time (used 400 normalized iris images) for feature extraction (from normalized iris image to features vector) and matching (including rotation invariance schemes) is given in the following table (table 1). Whereas, we present the different error rates given by our experimental results in the Table 2.

Table 1: Average computational time of different algorithms

Method	Feature extraction (ms)	Matching (ms)	Total (ms)	Length of feature Vector
Daugman	300.21	7.45	312.26	2,048-bits
Our proposed method	109	1.2	110.2	648 integer values

From the point of view complexity, as shown in Table 1, our proposed method clearly outperforms the other method. In particular, it can be said that, our proposed method is about 2.83 times faster. It is worth noting that the speed results were obtained on a PC running Windows OS with a 2.3 MHz clock speed and the implementations were carried out under MATLAB tools.

Table 2 Recognition accuracy and error rates of different iris algorithms on CASIA-Iris V1.0 and CASIA-Iris V2.0 databases

Database	CASIA_Iris V1.0		CASIA_Iris V2.0 (device1)	
	Daugman	Our proposed method	Daugman	Our proposed method
FRR	0.83	2.78	1.87	0.64
FAR	0.71	2.65	1.45	0.69
recognition rate	99.07	97.22	98.13	99.35
ERR	0.77	2.71	1.66	0.67

From the point of view performance and by comparing our method with Daugman's method, as shown in Table 2, our proposed method clearly made an encouraging result. The evaluation on the Casia Version 1 database, Daugman's method achieves a slightly better recognition rate (+1.85%). But, our method gave excellent results by evaluating on the basis of Casia version 2 (device 1) database, the Equal Error Rate (ERR) is only 0.67%. These results are quite encouraging and indicate the high performance of the proposed method. In addition, our method achieves a slightly better recognition rate (+1.22). While being evaluating our method on the iris CasiaV1 database, our method gave a false acceptance rate (FAR) of 2.65% and a false rejection rate (FRR) of 2.78% while in the evaluation on the basis of iris CasiaV2 database, the FAR of our method is only 0.69% and the FRR is 0.64%. Thus, we can conclude that our iris verification method based on curvelet transform is one of the successful iris verification.

V. CONCLUSION

Our proposed iris verification method based on curvelet transform has demonstrated to be promising for iris recognition. The method decomposes the iris in a set of sub-bands images, and then calculates some statistical features of such sub-band to represent the normalized iris. Through various experiments, we show that the proposed iris features extraction method can be used for personal verification systems in an efficient way.

REFERENCES

- [1] C.Sanchez-Avila a ,R.Sanchez-Reillo , Two different approaches for iris recognition using Gabor filters and multiscale zero-crossing representation, Pattern Recognition 38 (2005)231 .240
- [2] Amir Azizi and Hamid Reza Pourreza, A Novel Method Using Contourlet to Extract Features for Iris Recognition System,ICIC 2009, LNCS 5754, pp. 544–554, 2009.
- [3] W.W.Boles, B.Boashash,A human verification technique using images of the iris and wavelet transform,IEEE Trans.Signal Process.46 (4)(1998)1185 .1188.
- [4] Candes J., "Ridgelets: theory and applications," *Ph.D. thesis*, Department of Statitics, Stanford University, 1998.
- [5] E. J. Candès and D. L. Donoho, "Curvelets—A surprisingly effective nonadaptive representation for objects with edges," in *Curve and Surface Fitting: Saint-Malo 1999*,A. Cohen, C. Rabut, and L. L. Schumaker, Eds. Nashville, TN: Vanderbilt University Press, 1999.
- [6] Candès. Emmanuel, Demanet. Laurent and Donoho.David ,etal , "Fast Discrete Curvelet Transforms". Multiscale Modeling and Simulation, 5 (3). pp. 861-899,2006.
- [7] J. Daugman, High Confidence Visual Recognition of Persons by a Test of Statistical Independence, IEEE Trans. Pattern Analysis and Machine Intelligence, vol. 15, no. 11, pp. 1148-1161, Nov. 1993.

- [8] Haralick, R.M., Shanmugam, K., Stein, L.D.: Textural features for image classification. IEEE Transactions on Systems, Man, and Cybernetics 3(6), 610–621 (1973)
- [9] Khin Sint Sint Kyaw, Iris Recognition System using statistical features for Biometric Verification, 2009 International Conference on Electronic Computer Technology
- [10] Peter Kovesi. Matlab functions for computer vision and image analysis. 2004. <http://cs.uwa.edu.au/~pk/Research/MatlabFns/>
- [11] Majumdar, A.: Bangla basic character recognition using digital Curvelet transform. J. Pattern Recogn. Res. 2(1), 17–26 (2006)
- [12] Tanaya Mandal, Q.M.J.Wu. "Face Recognition using Curvelet Based PCA". In: ICPR, 2008.
- [13] Libor Masek. Recognition of human iris patterns for biometric identification. 2003. <http://www.csse.uwa.edu.au/~pk/studentprojects/labor>
- [14] Makram Nabti, Ahmed Bouridane. Wavelet Maxima and Moment Invariants Based Iris Feature Extraction. ICIP (2)2007. pp.397~400
- [15] Semler, L., & Dettori, L. A Comparison of Wavelet-Based and Ridgelet-Based Texture Classification of Tissues in Computed Tomography. Proceedings of International Conference on Computer Vision Theory and Applications, (2006).
- [16] Sumana, I.J., Islam, M.M., Zhang, D., Lu, G.: Content based image retrieval using Curvelet transform. In: Proceedings of IEEE International workshop on multimedia signal processing, MMSP08, pp. 11–16 (2008)
- [17] WANG Tong et HE Pi-Lian A Hidden Markov Model For Iris Recognition Method, 2007 IEEE International Conference on Control and Automation Guangzhou, CHINA - May 30 to June 1, 2007
- [18] R. Wildes, J. Asmuth, S. Hsu, R. Kolczynski, J. Matey, and S. McBride, Automated, Noninvasive Iris Recognition System and Method, United States Patent, no. 5572596, 1996
- [19] F. Rossant, M. Torres Eslava, T. Ea, F. Amiel, A. Amara, Iris identification and robustness evaluation of a wavelet packets based algorithm, IEEE International Conference on Image Processing (ICIP), Vol. 3. pp. 257-260, Genova, Italy, 2005.
- [20] CASIA-Iris. <http://biometrics.idealtest/>